Metallation-induced heterogeneous dynamics of DNA revealed by single-molecule FRET

Raul Berrocal-Martin,[a] Carlos Sanchez-Cano,[b] Cookson K. C. Chiu,[b] Russell J. Needham,[b] Peter J. Sadler[b,*] and Steven W. Magennis[a,*]

[a] School of Chemistry, University Avenue, University of Glasgow, G12 8QQ, UK

[b] Department of Chemistry, University of Warwick, Gibbet Hill, Coventry, CV4 7AL

Corresponding Author

*E-mail: steven.magennis@glasgow.ac.uk; p.j.sadler@warwick.ac.uk

The metallation of nucleic acids is key to wide-ranging applications, from anticancer medicine to nanomaterials, yet there is a lack of understanding of the molecular-level effects of metallation. Here, we apply single-molecule fluorescence methods to study the reaction of an organo-osmium anticancer complex and DNA. Individual metallated DNA hairpins are characterized using Förster resonance energy transfer (FRET). Although ensemble measurements suggest a simple two-state system, single-molecule experiments reveal an underlying heterogeneity in the oligonucleotide dynamics, attributable to different degrees of metallation of the GC-rich hairpin stem. Metallated hairpins display fast two-state transitions with a two-fold increase in the opening rate to ~2 s^{-1}, relative to the unmodified hairpin, and relatively static conformations with long-lived open (and closed) states of 5 s to ≥ 50 s. These studies show that a single-molecule approach can provides new insight into metallation-induced changes in DNA structure and dynamics.

The interaction of metal ions (*e.g.* K^+, Na^+ and Mg^{2+}) with nucleic acids is essential for many biological processes such as ion-mediated folding.[1] In contrast, transition metals can catalyse DNA damage via oxidative pathways, resulting in cell toxicity.[2] DNA is also a target

site for several transition metal anticancer complexes. Best known are the clinical drugs cisplatin,[3] and carboplatin, which form a range of DNA adducts, inducing structural changes that ultimately lead to the initiation of cell death mechanisms via apoptosis.[4] Furthermore, other metal-based drug candidates have also been designed to interact with DNA, leading to lesions that are different to those formed by clinical platinum drugs, potentially overcoming platinum resistance.[5] Beyond their biological role, metal-nucleic acid interactions are important in DNA-based sensors for metal ions [6] and as structural elements in DNA nanoscience, where metal-mediated base pairs (*e.g.* Ag^{+}, Cu^{2+}, Hg^{2+}) control the assembly of supramolecular structures (often using modified nucleobases).[7] Utilizing and optimizing such metal-DNA interactions requires knowledge of the structure and dynamics of the complexes formed.

In this context, the study of metal-DNA interactions at the single-molecule level can provide unique information otherwise inaccessible to commonly used bulk methods.[8] For example, single-molecule techniques can reveal, in a direct manner, static heterogeneity in molecular ensembles, without any *a priori* assumptions of the underlying distribution. Furthermore, dynamics can be monitored directly, without the need for synchronization of the molecular ensemble (*e.g.* pump-probe methods). As such, the effect of essential cations (e.g. Na^{+} and Mg^{2+}) on the folding of nucleic acids has been extensively explored using various single molecule approaches, including fluorescence and force methods.[9] Fluorescence-based methods have also been used to study metal binding to DNA modified by ligands capable of chelating copper ions[10] In contrast, only a few studies exploring the direct metalation of DNA at the single molecule level have been reported to date; mostly using single-molecule force spectroscopy such as optical and magnetic tweezers, and AFM. [11]

Here we employ single-molecule Förster resonance energy transfer (FRET) imaging, which is ideal for probing nanoscale structure and dynamics,[12] to study the direct interaction of the metal complex **Os1-Cl** with an unmodified DNA hairpin, as a model system (Figure 1). **Os1-Cl** belongs to a promising class of organometallic anticancer drugs: ruthenium or osmium-

based pseudo-octahedral half-sandwich complexes of the type $[(\eta^6\text{-arene})Ru/Os(N,N)Cl]^+$, containing a π-bonded arene *e.g.* p-cymene or biphenyl, and an *N,N*-chelated diamine such as ethylenediamine. [13] Such Ru and Os drug candidates have shown high activity against cisplatin-resistant cell lines.[14] However, in contrast to cisplatin, these complexes have only one reactive M-Cl bond, and can form only monofunctional adducts with DNA.[14] Interestingly, high-resolution mass spectrometry has shown that **Os1-Cl** can bind strongly to both guanine and cytosine residues on DNA oligonucleotides (upon hydrolysis of the Os-Cl bond).[15] Furthermore, the ruthenium analogue has been shown to form di-metallated adducts with hydrophobic interactions between the arene ligands in neighboring nucleobase sites; these DNA lesions are distinct structurally from cross-linked platinated adducts.[16]

In this work, we have studied the metallation of native DNA using single-molecule FRET. This reveals the presence of sub-populations that are not apparent from the equivalent ensemble measurements, and allows direct measurement of metallation-induced changes in the dynamics of DNA hybridization (millisecond to second timescale). The single-molecule experiments provide new insight into the structural perturbations of the oligonucleotide introduced upon binding to the organo-osmium anticancer complex.

Results

To investigate the interaction of organo-osmium anticancer complex **Os1-Cl** with DNA, we employed a DNA hairpin consisting of two single-stranded oligonucleotides (H1 and H2/H3; see Supporting Information, Methods and Materials), with a 20 nucleotide double-stranded handle, a 32 nucleotide polyA loop, and a stem region of 6 base pairs (5 GC and 1 AT; Figure 1).[17] Hairpins are excellent probes for DNA hybridization.[18] The hairpin used here was labeled with fluorophores acting as a donor:acceptor couple, with either Cy3 (H1-Cy3) or Cy3B (H1-Cy3B) as the donor, and Cy5 (H2) as acceptor (Fig. 1). This is expected to generate a low FRET signal when the hairpin stem is open (unpaired) and a high signal when the stem is closed

(paired).[17] Furthermore, the system carries a biotin moiety, which allowed the hairpin to be immobilized on a PEG-functionalised coverslip for single molecule experiments. **Os1-Cl** is known to bind specifically to guanine and cytosine bases,[15] so the hairpin provides suitable target sites, particularly in the GC-rich stem. To investigate the effect of metallation reactions on the dynamic properties of the hairpin, pre-formed DNA hairpins and **Os1-Cl** were incubated at nucleotide:**Os1-Cl** mol ratios up to 1:1.6 in the dark at 37 °C for 3 days using a low-salt buffer (see Supporting Information, Methods and Materials).

Ensemble fluorescence spectroscopy

Steady-state fluorescence spectroscopy and time-correlated single-photon counting (TCSPC) were used to probe the interaction of **Os1-Cl** with the DNA hairpin at the ensemble level. Hairpin closing is favored at high salt concentrations because Na^+ ions neutralize the negative charge on the DNA backbone. We looked first at hairpins with Cy3B as the donor dye. In the absence of the osmium complex, the addition of NaCl resulted in a decrease of the steady-state intensity of the Cy3B emission and a corresponding increase in the emission from Cy5 (Figure 2a). As the excitation wavelength (λ_{ex} = 532 nm) corresponds to Cy3B absorption, we attribute these intensity changes to increased FRET following salt-induced hairpin closing (inset to Figure 2a). As expected for FRET, the intensity changes are matched by a decrease in the average donor lifetime (Figure 2d and Supporting Information, Table S1). The Cy3B lifetime is biexponential in the hairpin. The long decay component of 2.8 ns is similar to that of free Cy3B,[19] attributable to the open hairpin. The short decay component of ~0.35 ns is attributed to Cy3B undergoing FRET in the closed hairpin. As the salt concentration increases, the amplitude of the short component increases from 14% to 73% (Supporting Information, Table S1).

Then, the pre-formed DNA hairpin was mixed with **Os1-Cl** at different nucleotide:**Os1-Cl** mol ratios (1:0.8 or 1:1.6), and incubated in the dark at 37 °C for 3 days. Following incubation, samples were titrated with various NaCl concentrations (10-180 mM) and ensemble

fluorescence measurements were made (Figure 2 and Supporting Information, Tables S1 and S2). At a nucleotide:**Os1-Cl** ratio of 1:0.8, the steady-state FRET is greatly reduced (from 0.6 to 0.25 at 180 mM NaCl; Figure 2b) while at the higher ratio (1:1.6), FRET is 0.22, (Figure 2c) which is close to the low-salt control value of 0.18 (Figure 2a). As expected for a reduction in FRET, the absolute intensity of the donor emission increases in the presence of osmium; this increase is small at low salt but is substantial at high salt (Supporting Information, Figure S1).

In support of the assignment of reduced FRET, the average lifetime of the donor after incubation with the complex shows a smaller reduction at a given salt concentration for 1:0.8 in comparison to the control sample (Figure 2e and Supporting Information, Table S1); this is due to a decrease in the fraction of the short-lived population. For the 1:1.6 DNA:Os ratio, the increase of salt to 180 mM results only in an increase in the amplitude of the short decay component from 11% to 16% (Figure 2f and Supporting Information, Table S1). Furthermore, after incubation with **Os1-Cl**, there were still only two Cy3B decay components present. As previously observed in non-metallated controls, the long component is similar to free Cy3B alone (~2.7 ns), characteristic of the open hairpin. However, the short component is ~1 ns, indicating a less efficient energy transfer process for the closed state, in comparison to the complex-free control.

Similar experiments were performed using a donor-only (Cy3B) DNA hairpin incubated at 37 °C for 3 days with and without **Os1-Cl** (1:0, 1:0.8 and 1:1.6 nucleotide:**Os1-Cl**; Figure S2 and Supplementary Table 3). The steady-state intensity of Cy3B was almost unchanged in both the absence and presence of **Os1-Cl**. In the absence of the osmium complex, the Cy3B lifetime showed a slight enhancement from ~2.9 ns to ~3.2 ns as the [NaCl] was increased to 180 mM, which we attribute to local effects of the salt on the dye. However, this was not observed after incubation of the hairpin with **Os1-Cl**; the Cy3B lifetime was almost constant across the whole range of salt concentrations (~2.8 ns). Therefore there appears to be a small quenching effect due to the presence of the osmium complex that counter-acts the aforementioned local

enhancement due to the NaCl. Finally, direct excitation of Cy5 in the doubly-labelled hairpin showed very little change in either the steady-state spectra or lifetime of the acceptor after incubation of the hairpin with **Os1-Cl**, even at high [NaCl] (Figure S3 and Supplementary Table 4).

We next repeated our tests using Cy3 as a donor in place of Cy3B. Samples were excited at 532 nm, corresponding to Cy3 absorption. In general, the same results were obtained as for the Cy3B-labelled hairpins (Supporting Information, Tables S5 and S6, and Figures S4 and S5). The key difference with the experiments using Cy3-Cy5 hairpins is that the relative intensities of donor and acceptor differ from the hairpins labelled with Cy3B-Cy5 (Supporting Information, Table S5 and Figure S4). In addition to changes in the extent of energy transfer for the different donor dyes (e.g. due to Förster radius, dye-dye distance), we previously observed that Cy3 intensity increases upon hairpin closing due to stacking in the gap. [20] This was termed stacking-induced fluorescence increase (SIFI) and is due to the prevention of photoisomerisation upon stacking. For the donor-only hairpin, the interaction with **Os1-Cl** prevents closing and thus stacking, resulting in a decrease in Cy3 emission intensity as salt is increased (Supporting Information, Table S6 and Figure S5).[20] The other difference between experiments with Cy3 and Cy3B is that Cy3 displays three lifetime components, which are attributed to different local dye environments, as discussed previously.[20]

To investigate whether the **Os1-Cl** is targeting the GC-rich stem, a new hairpin (H4-Cy3) was designed with an AT-rich stem and similar thermodynamic stability as the GC-rich hairpin (Supporting Information, Figure S6). In the absence of the **Os1-Cl**, the addition of NaCl resulted in a decrease of the steady-state intensity of the Cy3 emission and a corresponding increase in the emission from Cy5 (Supporting Information, Figure S7 and Table S7). As observed for the GC-rich hairpin, **Os1-Cl** also suppresses the closing for hairpin H4-Cy3/H2, but the effect is much more pronounced for the GC-rich hairpin (Supporting Information, Figure S8).

Single-molecule FRET

The interaction between **Os1-Cl** and the DNA hairpin was further investigated using total internal reflection fluorescence (TIRF) microscopy to study single-molecule FRET. DNA samples were prepared as before by mixing the DNA hairpin with **Os1-Cl** in 1:0.5 and 1:1 nucleotide:**Os1-Cl** ratios and incubating in the dark at 37 °C for 3 days. The hairpin was then immobilized on a PEG-coated slide via biotin-neutravidin attachment chemistry. We used Cy3 as the donor and Cy5 as the acceptor, in order to compare our results directly with our previous single-molecule FRET experiments for this hairpin.[17] Single-molecule time traces of the donor and acceptor were recorded, allowing us to construct FRET time traces. From these we analyzed the distribution of FRET states of hundreds of single-molecules, and the state-to-state kinetics of individual trajectories.

In the absence of **Os1-Cl**, single-molecule FRET histograms composed from the raw time traces of *ca.* 200 molecules could be fitted as two FRET states (Figure 3 and Supporting Information, Figure S9 and Table S8). At low [NaCl] the hairpin was mostly in the low FRET state, but increasing [NaCl] led to the predominance of the high FRET state (Figure 3a and Supporting Information, Figure S9). For samples incubated with 0.5 or 1 equivalent of **Os1-Cl**, the same two states were still present, but the population of the high-FRET state was greatly reduced for any given [NaCl] (Figures 3b and 3c, and Supporting Information, Figure S9 and Table S8). This was particularly dramatic in samples prepared with 1:1 ratios (nucleotide:**Os1-Cl**), where the low-FRET state of the hairpin was always dominant. As such, FRET population histograms of DNA treated with 1 mol equiv. of the complex in the presence of 100 mM NaCl resembled that of untreated controls at low salt (Figure 3 and Supporting Information, Figure S9). The trends in low/high FRET population from single-molecule measurements as a function of **Os1-Cl** and salt (Supporting Information, Table S8) were very similar to those measured via ensemble TCPSC data (Supporting Information, Table S1). Importantly, direct excitation of the

Cy5 acceptor showed that hairpins displaying low FRET states still possessed an active Cy5 (Supporting Information, Figure S10), which ruled out that the low acceptor signal was due to the absence, quenching or bleaching of the acceptor dye.

The raw time traces for the DNA hairpin could be fitted to two FRET states in both the absence and presence of **Os1-Cl** (Figure 4a and 4b).[17] The fraction of hairpins open and closed, calculated from the time spent in the low and high FRET states, respectively (Figure 4c and 4d) are in good agreement with the Gaussian fits from the raw data (Figure 3 and Supporting Information, Figure S9). In general, the time-traces displayed anti-correlated FRET signals. The traces in the absence of **Os1-Cl** matched those seen previously (Figure 4a).[17] In the presence of **Os1-Cl**, the same two FRET states as in the complex-free sample were observed but the traces displayed both fast and slow dynamics (Figure 4b). The stable traces were predominately in the low FRET state, and the number of traces with long dwell times was larger when incubated with a higher concentration of **Os1-Cl**.

The fast fluctuation events had dwell times mostly below 5 s. These short dwell times dominated the dwell time distributions and could be fitted to a two-state model with a single exponential, with and without **Os1-Cl** (Figure 5). Rate constants determined in the absence of **Os1-Cl** (Figure 5a and 5d) agreed with those reported previously (*e.g.* in 40 mM NaCl: k_{open} = 1.1 s^{-1} and k_{close} = 4.2 s^{-1}).[17] Remarkably, the transition rate from low FRET to high FRET was unaffected by **Os1-Cl**, but there was an increase in the rate constant from the high- to low-FRET state from ~1 s^{-1} to ~2 s^{-1} when DNA was treated with the complex. The rate constants for these fast two-state dynamics do not agree with the total fraction of time spent in each of the two states (Figure 4). For example in 40 mM NaCl and 1:1 nucleotode:**Os1Cl** the short time dynamics fit to a closing rate of ~4 s^{-1} and an opening rate of ~2 s^{-1} (Figure 4c and 4d), which corresponds to a 2:1 ratio of closed:open hairpins. However, the fraction of time in the closed state versus the open state is closer to 1:3 closed:open (Figure 3 c and 3d). This discrepancy is resolved by comparing the fraction of time spent in each state for dwell times up to 5s

(Supporting Information, Table S9) with all dwell times from t=0s to the window size of t=50s (Supporting Information, Table S10). Some of the long-lived states were stable throughout the measurement window of 50 s and were mostly low FRET states, though stable high-FRET states were also observed. Some of the stable states also occasionally exhibited fast fluctuations to high intensity acceptor levels that were not accompanied by an anti-correlated decrease in donor intensity (*e.g.* see Supporting Information, Figure S11).

Discussion

We studied the interaction of the organo-osmium(II) arene anticancer complex **Os1-Cl**, with a DNA hairpin using ensemble and single-molecule FRET. The ensemble FRET measurements support a simple model of two-state hairpin opening and closing, with the complex reducing the fraction of the closed (high FRET) state, and leaving most hairpins in the open (low FRET) state. Control samples showed that changes in FRET are due to changes in hairpin structure, and not local dye effects, and the population of the high FRET state increases at high [NaCl]. Overall, the ensemble results are in agreement with NaCl-dependent opening and closing reported previously for similar hairpins using FRET.[17] We hypothesize that the **Os1-Cl** is binding to the GC-rich hairpin stem. To test this we compared GC-rich and AT-rich hairpins that had similar thermodynamic stability. The extent of hairpin opening was much less for the AT-rich hairpin, despite having almost double the number of bases available for binding in the stem region (11 AT pairs versus 1AT and 5 GCs). This agrees with earlier published work, which showed that **Os1-Cl** binds more strongly to Gs and Cs than to As and Ts.[15]

Detailed examination of the time-traces of individual immobilized DNA hairpins revealed state-to-state kinetics that were not apparent from either the bulk measurements or the FRET histograms. Single-molecule FRET histograms of immobilized hairpins (Figure 3), before and

after incubation with **Os1-Cl**, appeared to support the ensemble results. However, examination of the time traces of individual hairpins over the whole measurement window revealed a rich dynamic behavior, which was hidden at the bulk level. Although the hairpin appears to adopt only two major conformations (open and closed), resulting in two FRET states (low and high, respectively) the data cannot be modelled as a simple two-state system. Instead, there is significant heterogeneity in the dynamics. The time traces can be split into (at least) two classes: fast dynamics that can fitted to a two-state model, and a series of more static open (and to a lesser extent closed) conformations. Both types of dynamics must be accounted for, in order to agree with the ensemble measurements.

Under the low salt concentrations used during the incubation of the hairpin with **Os1-Cl**, it is likely that most of the complex is (**Os1-OH_2)**; where the chloride ligand is exchanged for a water molecule.[14] [21] Guanine and cytosine bases are known to bind strongly to **Os1-OH_2**.[15] There are 10 G and C bases in the stem region of our hairpin, so these bases are likely targets. Interestingly, previous bulk studies showed high levels of DNA unwinding induced by **Os1-Cl**.[14] They also suggested that the biphenyl arene ligand can interact with DNA via non-covalent intercalation between the bases,[14] which explained why substitutions on this ligand modulated the cytotoxicity.[22] Furthermore, π-π stacking interactions between arene ligands on neighbouring complexes were observed,[15] affecting significantly fragmentation of the oligonucleotide during MS experiments, and suggesting that interaction between arene ligands on bound **Os1** moieties could alter not only DNA structure, but also its hybridization dynamics.

This explanation agrees with the results obtained from our single molecule FRET experiments, which demonstrate that binding of the complex causes a major disruption of secondary structure. We attribute the heterogeneous dynamic behaviour to variations in the number of complexes bound to the hairpin. Many hairpins can open and close in a similar fashion to the unmodified hairpin, albeit with an increased opening rate. We assign these as hairpins with low numbers of bound complexes. Interestingly, thermodynamic calculations

suggest that disruption of a single base pair in the middle of the stem region might be enough to destabilize the hairpin at room temperature (see Supporting Information, Figures S12-14). As the degree of metalation increases, hairpins might be locked in the open and closed conformations for much longer times. This may be due to the cumulative effects of multiple bound complexes and/or from interactions between ligand and DNA or ligand-ligand interactions.[16] In this context, it is likely that our separation into short and long dwell-time behavior is an oversimplification. Furthermore, some time-traces do not follow simple anti-correlated FRET behavior. Some of the fast fluctuations observed could be due to local interactions between the dyes and **Os1** (e.g. via interactions with the biphenyl ligand).

Overall, this work provides important new insights into the heterogeneous dynamic effects on a DNA oligonucleotide hairpin induced by metallation by an osmium anticancer complex. Our experiments also demonstrate the power of fluorescence-based single-molecule methods to study the interaction of metals with DNA and/or other biomolecules, as they are capable of providing unique information on dynamic processes and reveal complexity in apparently simple bulk systems.

Acknowledgements

We thank the EPSRC (PhD studentships for RBM and CKCC, Grant no. EP/P030572/1), CRUK/EPSRC (Grant No. C53561/A19933), The Wellcome Trust (Grant No. 107691/Z/15/Z), and AngloAmerican for support.

AUTHOR INFORMATION

Corresponding Author

steven.magennis@glasgow.ac.uk, P.J.Sadler@warwick.ac.uk

The authors declare no competing financial interests.

References

[1] *Nucleic Acid-Metal Ion Interactions* (Ed.: N. V. Hud), RSC Publishing, **2009**.

[2] C. J. Burrows, J. G. Muller, *Chem. Rev.* **1998**, *98*, 1109-1151.

[3] a) B. Rosenberg, L. Vancamp, T. Krigas, *Nature* **1965**, *205*, 698-699; b) B. Rosenberg, L. Vancamp, J. E. Trosko, V. H. Mansour, *Nature* **1969**, *222*, 385-386.

[4] a) J. M. Pascoe, J. J. Roberts, *Biochem. Pharmacol.* **1974**, *23*, 1345-1357; b) A. W. Prestayko, J. C. Daoust, B. F. Issell, S. T. Crooke, *Cancer Treatment Reviews* **1979**, *6*, 17-39; c) B. Wu, P. Droge, C. A. Davey, *Nat. Chem. Biol.* **2008**, *4*, 110-112; d) A. I. Minchinton, I. F. Tannock, *Nat. Rev. Cancer* **2006**, *6*, 583-592.

[5] a) S. M. Meier-Menches, C. Gerner, W. Berger, C. G. Hartinger, B. K. Keppler, *Chem. Soc. Rev.* **2018**, *47*, 909-928; b) C. A. Riedl, L. S. Flocke, M. Hejl, A. Roller, M. H. M. Klose, M. A. Jakupec, W. Kandioller, B. K. Keppler, *Inorg. Chem.* **2017**, *56*, 528-541; c) B. Wu, M. S. Ong, M. Groessl, Z. Adhireksan, C. G. Hartinger, P. J. Dyson, C. A. Davey, *Chem. Eur. J.* **2011**, *17*, 3562-3566; d) A. M. Pizarro, N. P. E. Barry, P. J. Sadler, in *Comprehensive Inorganic Chemistry II, Vol. 3* (Eds.: J. Reedijk, K. Poeppelmeier), Elsevier, Oxford, **2013**, pp. 751-784.

[6] a) T. Hong, Y. Yuan, T. Wang, J. Ma, Q. Yao, X. Hua, Y. Xia, X. Zhou, *Chem. Sci.* **2017**, *8*, 200-205; b) B. Jash, P. Scharf, N. Sandmann, C. F. Guerra, D. A. Megger, J. Mueller, *Chem. Sci.* **2017**, *8*, 1337-1343.

[7] a) G. H. Clever, C. Kaul, T. Carell, *Angew. Chem. Int. Ed.* **2007**, *46*, 6226-6236; b) B. Jash, J. Mueller, *Chem. Eur. J.* **2017**, *23*, 17166-17178; c) D. M. Engelhard, J. Nowack, G. H. Clever, *Angew. Chem. Int. Ed.* **2017**, *56*, 11640-11644.

[8] W. E. Moerner, *Angew. Chem. Int. Ed.* **2015**, *54*, 8067-8093.

[9] a) R. Borner, D. Kowerko, H. G. Miserachs, M. F. Schaffer, R. K. O. Sigel, *Coord. Chem. Rev.* **2016**, *327*, 123-142; b) S. A. McKinney, A. C. Déclais, D. M. J. Lilley, T. Ha, *Nat. Struct. Biol.* **2003**, *10*, 93-97.

[10] a) D. Brox, A. Kiel, S. J. Woerner, M. Pernpointner, P. Comba, B. Martin, D.-P. Herten, *Plos One* **2013**, *8*; b) A. Kiel, J. Kovacs, A. Mokhir, R. Kraemer, D.-P. Herten, *Angew. Chem. Int. Ed.* **2007**, *46*, 3363-3366.

[11] a) A. A. Almaqwashi, T. Paramanathan, I. Rouzina, M. C. Williams, *Nucleic Acids Res.* **2016**, *44*, 3971-3988; b) I. D. Vladescu, M. J. McCauley, M. E. Nunez, I. Rouzina, M. C. Williams, *Nat. Methods* **2007**, *4*, 517-522; c) J. Camunas-Soler, M. Manosas, S. Frutos, J. Tulla-Puche, F. Albericio, F. Ritort, *Nucleic Acids Res.* **2015**, *43*, 2767-2779; d) A. Mihailovic, L. Vladescu, M. McCauley, E. Ly, M. C. Williams, E. M. Spain, M. E. Nunez, *Langmuir* **2006**, *22*, 4699-4709; e) X.-M. Hou, X.-H. Zhang, K.-J. Wei, C. Ji, S.-X. Dou, W.-C. Wang, M. Li, P.-Y. Wang, *Nucleic Acids Res.* **2009**, *37*, 1400-1410.

[12] a) T. Ha, T. Enderle, D. F. Ogletree, D. S. Chemla, P. R. Selvin, S. Weiss, *Proc. Natl. Acad. Sci. USA* **1996**, *93*, 6264-6268; b) S. Kalinin, T. Peulen, S. Sindbert, P. J. Rothwell, S. Berger, T. Restle, R. S. Goody, H. Gohlke, C. A. M. Seidel, *Nat. Methods* **2012**, *9*, 1218-1225; c) E. Lerner, T. Cordes, A. Ingargiola, Y. Alhadid, S. Chung, X. Michalet, S. Weiss, *Science* **2018**, *359*, 288.

[13] a) A. F. A. Peacock, A. Habtemariam, R. Fernandez, V. Walland, F. P. A. Fabbiani, S. Parsons, R. E. Aird, D. I. Jodrell, P. J. Sadler, *J. Am. Chem. Soc.* **2006**, *128*, 1739-1748; b) A. F. A. Peacock, S. Parsons, P. J. Sadler, *J. Am. Chem. Soc.* **2007**, *129*, 3348-3357; c) Z. Adhireksan, G. E. Davey, P. Campomanes, M. Groessl, C. M. Clavel, H. J. Yu, A. A. Nazarov, C. H. F. Yeo, W. H. Ang, P. Droge, U. Rothlisberger, P. J. Dyson, C. A.

Davey, *Nat. Commun.* **2014**, *5*; d) H. M. Chen, J. A. Parkinson, R. E. Morris, P. J. Sadler, *J. Am. Chem. Soc.* **2003**, *125*, 173-186; e) H.-K. Liu, S. J. Berners-Price, F. Wang, J. A. Parkinson, J. Xu, J. Bella, P. J. Sadler, *Angew. Chem. Int. Ed.* **2006**, *45*, 8153-8156; f) H.-K. Liu, J. A. Parkinson, J. Bella, F. Wang, P. J. Sadler, *Chem. Sci.* **2010**, *1*, 258-270.

[14] H. Kostrhunova, J. Florian, O. Novakova, A. F. A. Peacock, P. J. Sadler, V. Brabec, *J. Med. Chem.* **2008**, *51*, 3635-3643.

[15] C. A. Wootton, C. Sanchez-Cano, H.-K. Liu, M. P. Barrow, P. J. Sadler, P. B. O'Connor, *Dalton Trans.* **2015**, *44*, 3624-3632.

[16] H.-K. Liu, H. Kostrhunova, A. Habtemariam, Y. Kong, R. J. Deeth, V. Brabec, P. J. Sadler, *Dalton Trans.* **2016**, *45*, 18676-18688.

[17] L. E. Baltierra-Jasso, M. J. Morten, L. Laflor, S. D. Quinn, S. W. Magennis, *J. Am. Chem. Soc.* **2015**, *137*, 16020-16023.

[18] Y. Yin, X. S. Zhao, *Acc. Chem. Res.* **2011**, *44*, 1172-1181.

[19] M. E. Sanborn, B. K. Connolly, K. Gurunathan, M. Levitus, *J. Phys. Chem. B* **2007**, *111*, 11064-11074.

[20] M. J. Morten, S. G. Lopez, I. E. Steinmark, A. Rafferty, S. W. Magennis, *Nucleic Acids Res.* **2018**, *46*, 11618-11626.

[21] Y. Hung, W. J. Kung, H. Taube, *Inorg. Chem.* **1981**, *20*, 457-463.

[22] S. H. van Rijt, A. Mukherjee, A. M. Pizarro, P. J. Sadler, *J. Med. Chem.* **2010**, *53*, 840-849.

FIGURES

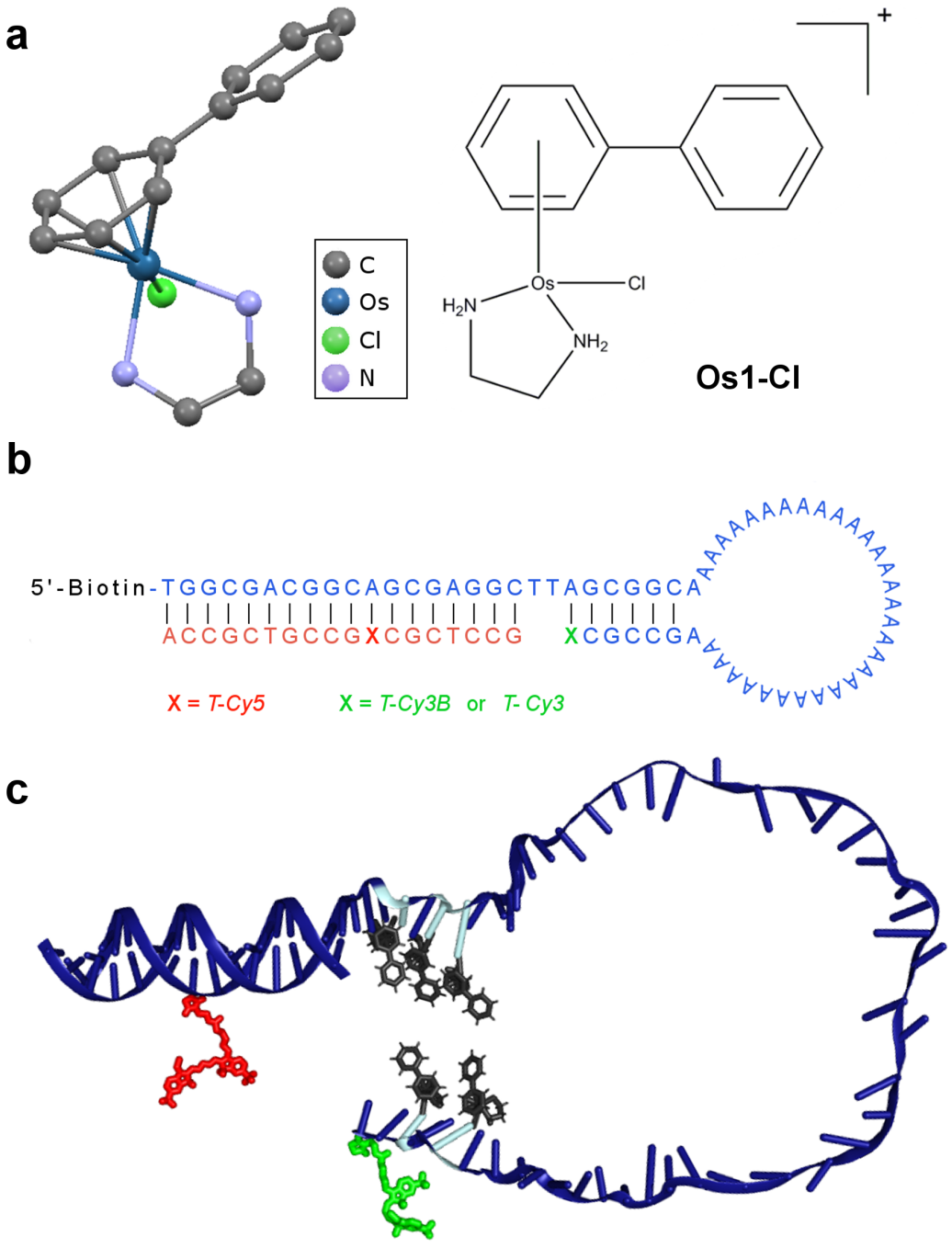

Figure 1 (**a**) The structure of **Os1-Cl**.[14] (**b**) The sequence and dye positions for the DNA hairpin. **c)** Illustration of multiple **Os-1** complexes bound to the GC-rich stem of the DNA hairpin inhibiting hairpin closing.

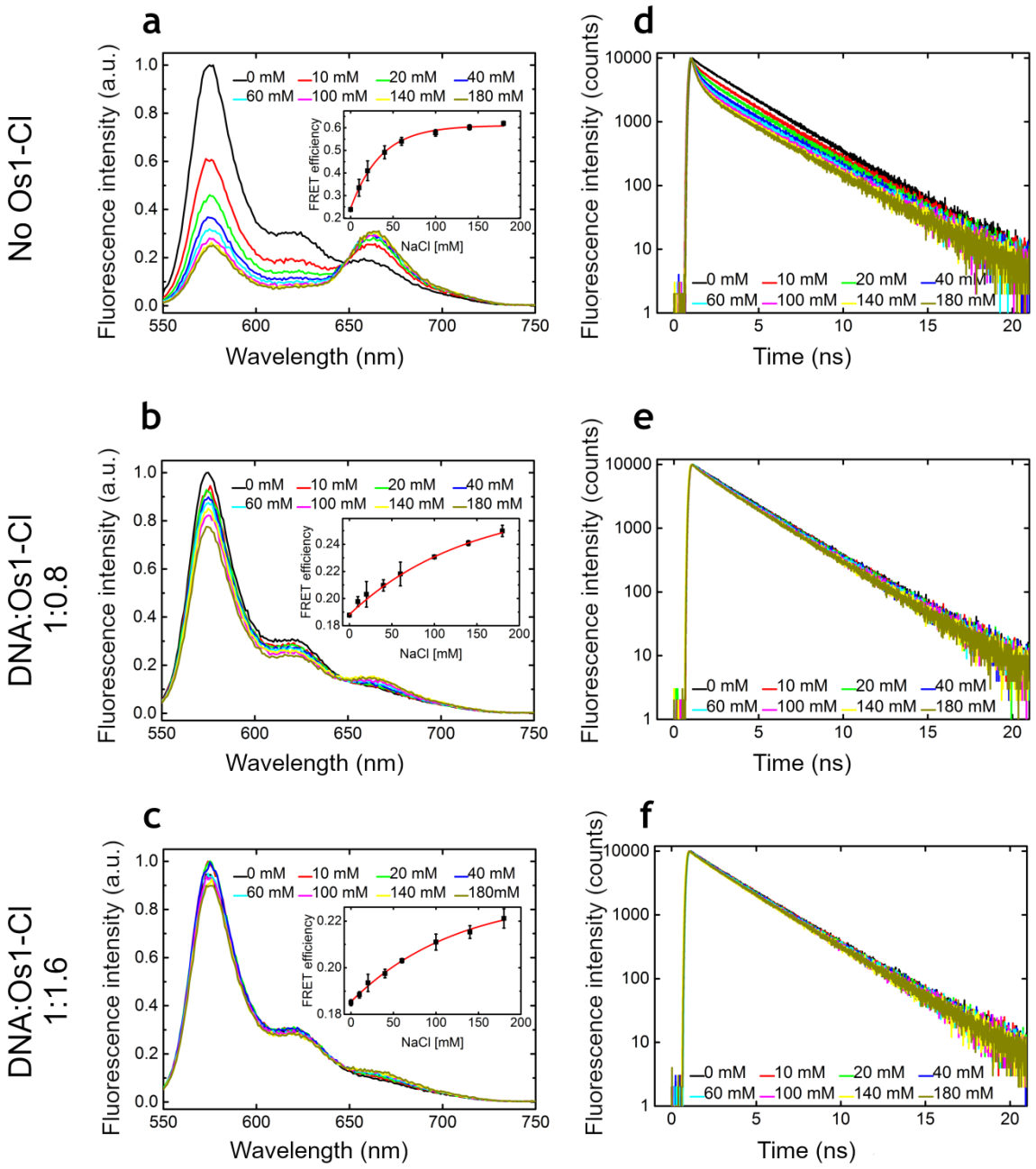

Figure 2 Ensemble fluorescence spectroscopy of DNA hairpin in the absence and presence of Os1-Cl as a function of the increase in [NaCl]. Steady-state (**a**, **b** and **c**) and time-resolved fluorescence (**d**, **e** and **f**) for the DNA hairpin (H1-Cy3B/H2) in the absence of **Os1-Cl** (top) and after incubation in the presence of **Os1-Cl** (1:0.8, middle; 1:1.16, bottom). The inset of **a-c** shows the FRET efficiency (see Supporting Information, Methods and Materials); the red line is a guide to the eye. The concentration for NaCl during incubation was ≤ 0.5 mM.

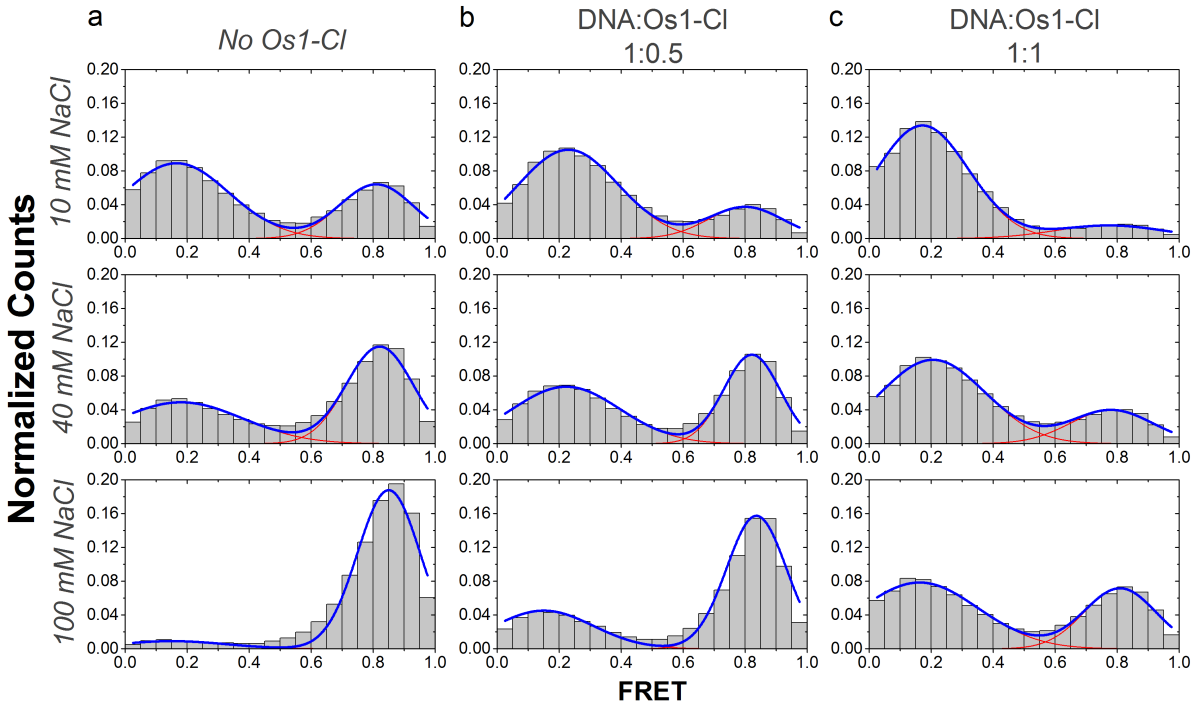

Figure 3 Single-molecule FRET of DNA hairpins in the absence and presence of Os1-Cl. DNA hairpin (H1-Cy3/H2) in the absence of **Os1-Cl** (**a**), and after incubation in the presence of **Os1-Cl** (1:0.5, **b**; 1:1, **c**). Data are shown for three concentrations of NaCl (10 mM, top; 40 mM middle; 100 mM, bottom). These graphs are directly extracted from the time traces of all FRET-active molecules (*ca*. 200 molecules). See Supporting Information (Table S8) for details of curve fitting.

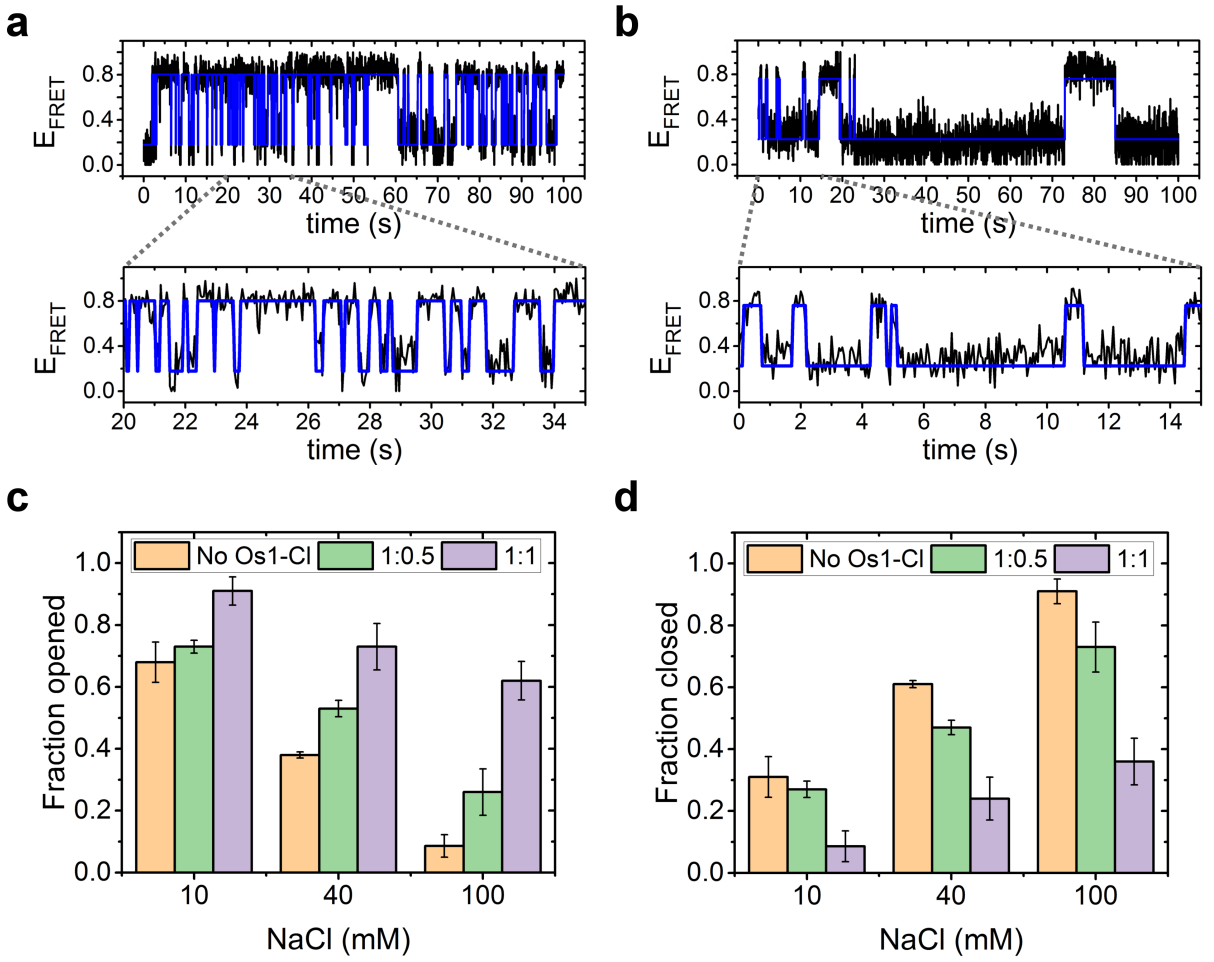

Figure 4 Single-molecule FRET time-traces of DNA hairpins in the absence and presence of Os1-Cl. Single-molecule FRET time-traces of DNA hairpins in the absence and presence of **Os1-Cl**. FRET traces for DNA hairpins (H1-Cy3/H2) in the absence of **Os1-Cl** (a) and after incubation in the presence of 1:1 DNA:**Os1-Cl** (b) are shown; the buffer contains 40 mM NaCl. The traces display only two FRET levels. The blue lines are the fits of a two-state analysis. The fraction of time spent in the open (c) and closed (d) conformation as a function of DNA:**Os1-Cl** and [NaCl] are extracted from the two-state fitting. Note that these time traces are selected from several individual time traces that have been stitched together for dwell-time analysis

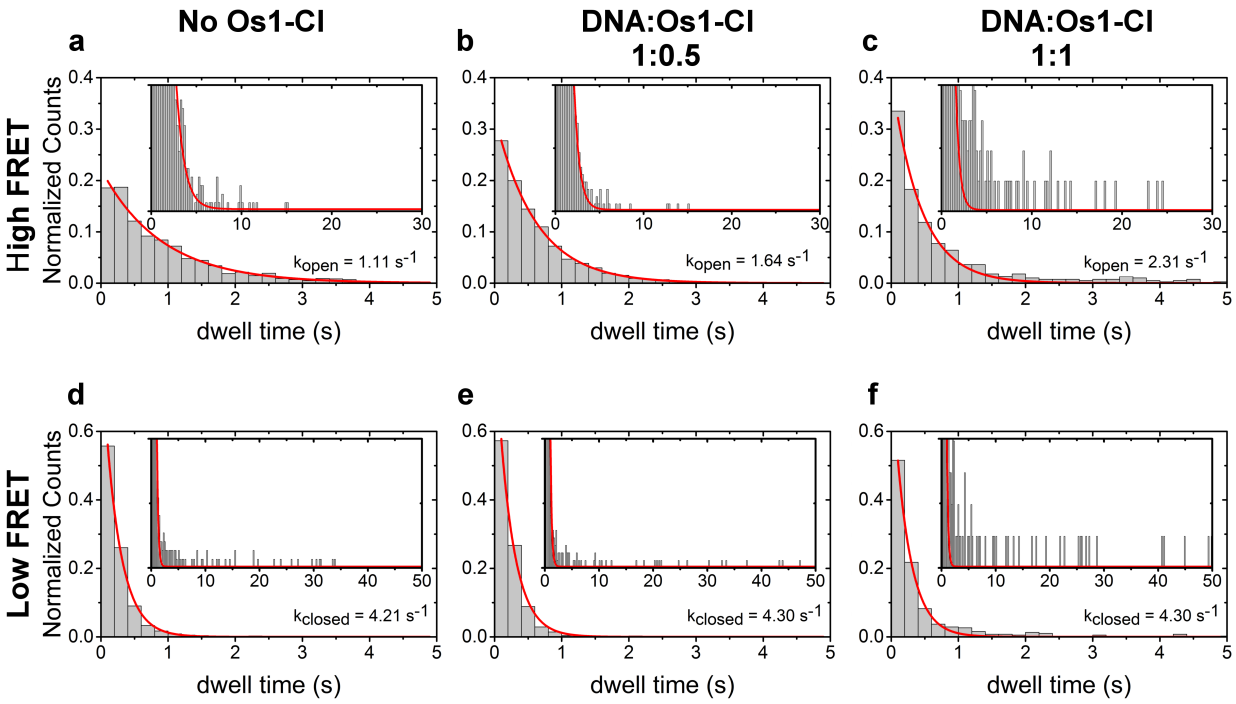

Figure 5. Hairpin dynamics in the absence and presence of Os1-Cl. Dwell time data in the closed, high FRET, state (a-c) and open, low FRET, state (d-f) are shown. Dwell time analysis for the DNA hairpin (H1-Cy3/H2) alone (a and d) or in the presence of 1:0.5 **Os1-Cl** (b and e) or 1:1 **Os1-Cl** (c and f) are shown. The buffer contains 40 mM NaCl. The inset shows fluctuations events for dwell times below 30 s (inset a-c) and 50 s (inset d-f) for the same closed (a-c) and open states (d-f) in the absence (a and d) or the presence of **Os1-Cl** at ratio 1:0.5 (b and e) and 1:1 (c and f).

Graphical Abstract

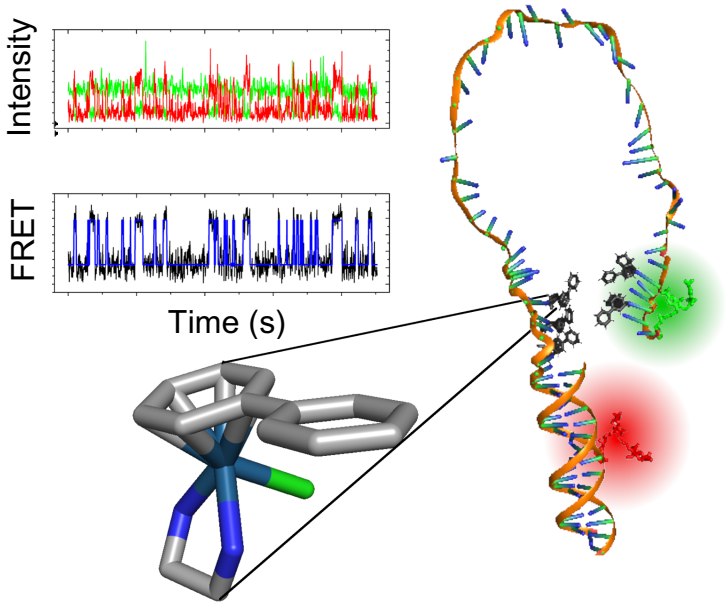

Dynamic complexity: The metallation of DNA by an organo-osmium anticancer complex is studied using single-molecule Förster resonance energy transfer (FRET), revealing dynamic heterogeneity that is obscured at the ensemble level.